Influence of Core Fucosylation on the Flexibility of a Biantennary N-Linked Oligosaccharide†

Hilary J. Stubbs,‡,§ Jiin J. Lih,|| Terry L. Gustafson,|| and Kevin G. Rice*,‡,§

Division of Pharmaceutics and Pharmaceutical Chemistry, College of Pharmacy and the Department of Chemistry, Ohio State University, Columbus, Ohio 43210

Received June 16, 1995; Revised Manuscript Received September 8, 1995⊗

ABSTRACT: Fluorescence energy transfer was used to study the conformation of each antenna of a complex biantennary oligosaccharide. A core fucosylated biantennary oligosaccharide was converted to a glycosylamine which allowed coupling of a naphthyl donor fluorophore directly to the reducing-end GlcNAc 1. After generating an aldehyde at C-6 of residue 6 or 6′ using galactose oxidase, a dansyl ethylenediamine acceptor fluorophore was coupled to either antenna of the oligosaccharide resulting in two donor−acceptor pairs.

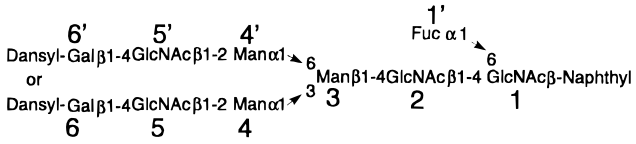

The fluorescence properties of the naphthyl group allowed determination of the end-to-end donor−acceptor distance and antenna flexibility of each isomer by steady-state and time-resolved fluorescence energy transfer at temperatures ranging from 0 to 40 °C. Extended (20.6 Å) and folded (11.4 Å) donor−acceptor distance populations were identified for the isomer containing dansyl attached to Gal 6′, whereas only a single extended population (19.7 Å) was determined when dansyl was attached to Gal 6. The presence of Fuc 1′ had a dramatic effect on the conformation of the 6′ antenna. Temperature modulation failed to alter the ratio of extended/folded populations when fucose was present. However, following the removal of fucose, the ratio of the extended/folded populations for 6′ exhibited a temperature dependent conformational equilibrium allowing calculation of the enthalpy and entropy of unfolding. These results established a unique conformational property for the 6′ antenna of a biantennary oligosaccharide that is influenced by core fucosylation. Comparison of the results obtained for the 6 antenna of biantennary with previous fluorescence energy transfer studies on a triantennary glycopeptide also established conformational differences in this antenna which are dependent on oligosaccharide structure.

N-linked oligosaccharides found on glycoproteins are ligands for plant and animal lectins (Lee, 1992; Sharon, 1993). Due to the potential for flexibility about glycosidic linkages the conformational requirements for efficient binding of an oligosaccharide ligand to a lectin are difficult to analyze. Presumably, the underlying pentasaccharide core structure found in all eukaryotic N-linked oligosaccharides serves as a scaffolding. Flexible glycosidic linkages within the core position the terminal sugar residues on the antennae into the proper orientation for binding to multiple, spatially resolved, binding sites on separate subunits of C-type lectins in mammals (Rice & Lee, 1990; Childs et al., 1990). Therefore, antenna flexibility could serve a specific role in directing precise recognition in carbohydrate−protein binding interactions. Alternatively, antenna flexibility may also serve less specific roles in protecting a glycoprotein from proteolysis or modifying protein conformation and function (Sharon, 1984).

Of the methods that have been used to investigate oligosaccharide conformation, only X-ray crystallography has provided high-resolution conformations of receptor-bound oligosaccharides (Cygler et al., 1991; Bourne et al., 1992, 1994). In general, the conformation of receptor-bound oligosaccharides diverge slightly from the global minimum determined by molecular modeling (Cheetum et al., 1992; Weis et al., 1992). This induced fit is the result of flexible glycosidic linkages often found in the pentasaccharide core region of the oligosaccharide (Rice et al., 1994).

Computational methods applied to oligosaccharides predict the existence of multiple low-energy conformations which can interconvert rapidly (Imberty et al., 1989; Koča et al., 1995). However, computational limitations often preclude the use of a solvent cage, making it difficult to correlate computed conformations with those measured in solution (Tvaroska et al., 1990). Furthermore, conformations computed for di- or trisaccharides may not be relevant to the conformation of these sequences inserted into a branched

† This work was supported by NIH Grants DK45742 and GM48048 (K.G. R.) and instrumentation support by NSF (CHE-9108384).

* To whom correspondence should be addressed.

‡ College of Pharmacy.

§ Present address: College of Pharmacy, University of Michigan, 428 Church St. Ann Arbor, Michigan 48109-1065. Tel: (313)-763-1032. FAX: (313)-763-2022.

|| Department of Chemistry.

⊗ Abstract published in *Advance ACS Abstracts,* January 1, 1996.

oligosaccharide. This is evident from studies which show that the conformation about a single glycosidic linkage is influenced by the conformation about nearby or adjacent linkages (Mazurier et al., 1991).

Of the methods available to directly analyze the conformation of N-linked oligosaccharides in solution, nuclear magnetic resonance spectroscopy (NMR) has been used most extensively (Brisson & Carver, 1983; Homans et al., 1983; Homans & Rutherford, 1993; Rutherford et al., 1993). Distances between protons on nearby sugar residues can be determined from NOE measurements (Carver, 1991). However, the time scale of the NOE experiment only allows the calculation of an average interproton distance. Thereby, the conformation of flexible oligosaccharides deduced by NOE data may not bear any resemblance to the most favorable conformation in solution (Jardetsky, 1980).

Fluorescence energy transfer is an alternative method to NMR for measuring long range distances (10−100 Å) in biomolecules such as proteins, oligonucleotides, and oligosaccharides (Wu & Brand, 1994). The nanosecond time resolution afforded by time-resolved fluorescence energy transfer provides the unique opportunity to directly measure the population distribution of conformers arising from flexible glycosidic linkages in complex carbohydrates (Rice et al., 1991, 1993; Wu et al., 1991).

One of the limitations in applying fluorescence energy transfer is the difficulty in introducing two fluorophores into precise locations in oligosaccharides. In the present study, we have developed a new fluorophore-labeling strategy to derivatize oligosaccharides at the reducing end with a donor and the nonreducing end with an acceptor fluorophore. This approach was applied to generate fluorescent oligosaccharides that were used to study the flexibility of each antenna of a core fucosylated biantennary oligosaccharide using fluorescence energy transfer. The results demonstrate that a core fucose influences the conformational flexibility of one antennae of this biantennary oligosaccharide and illustrate how energy transfer can be used to decipher subtle difference in the flexibility of N-linked oligosaccharides. This study adds to a growing data base of oligosaccharide conformations determined by fluorescence energy transfer.

MATERIALS AND METHODS

N-Hydroxysuccinimide, galactose oxidase (EC 1.1.3.9), catalase (EC 1.11.1.6), and α-fucosidase (EC 3.2.1.51) were purchased from Sigma (St. Louis, MO). β-Galactosidase (EC 3.2.1.23) was purchased from Boehringer Mannheim (Indianapolis, IN), and β-acetyl hexosaminidase (EC 3.2.1.52) and α-mannosidase (EC 3.2.1.24) were purchased from V-Labs (Covington, LA). Dicyclohexylcarbodiimide was purchased from Eastman Kodak Co. (Rochester, NY). 2-Naphthylacetic acid was purchased from Aldrich (Milwaukee, WI), and dansyl ethylenediamine was purchased from Molecular Probes (Eugene, OR). Trifluoroacetic acid (TFA) was purchased from Pierce (Rockford, IL). Preparative reverse-phase chromatography was performed using a computer-interfaced HPLC equipped with two pumps (Model 2350) and a variable wavelength UV/vis detector (V4) (ISCO, Lincoln, NE). Analytical reverse-phase chromatography was performed using a single pump (Model 2350) with a gradient programmer (Model 2360) (ISCO, Lincoln, NE). Detection was by fluorescence using an F1050 HPLC fluorimeter (Hitachi Instruments Inc., San Jose, CA). Analytical RPHPLC[1] C-8 and C-18 columns (0.47 × 25 cm) were purchased from Rainin (Woburn, MA). Preparative C-18 RPHPLC columns (S5 ODS2, 25 × 1 cm and 25 × 2 cm) were purchased from Phase Separations (Norwalk, CT) and a PRP-1 polymeric reverse-phase column (30.5 × 0.7 cm) was purchased from Hamilton (Reno, NV). HPAEC chromatography was performed on a PA1 column (0.47 × 25 cm) with pulsed amperometric detection (PAD) using a Dionex carbohydrate analyzer (Sunnyvale, CA). Precoated silica gel TLC plates were purchased from Alltech (Deerfield, IL). Deuterium oxide and deuterated chloroform were purchased from Isotech Inc. (Miamisburg, OH).

Synthesis of 2-Naphthyl-N-Hydroxysuccinimide Ester. Dicyclohexylcarbodiimide (DCC, 4.0 g, 20 mmol) was added to a solution of *N*-hydroxysuccinimide (2.3 g, 20 mmol) in 220 mL of ethyl acetate. The reaction was initiated by the addition of 2-naphthylacetic acid (3.6 g, 20 mmol) and stirred overnight at room temperature. The ethyl acetate was removed by rotary evaporation, and the product was dissolved in chloroform and washed three times with water. The organic phase was dried over anhydrous magnesium sulfate and the chloroform was removed by rotary evaporation. A white solid was obtained in 94% yield. Thin layer chromatography of the product and 2-naphthylacetic acid with ethyl acetate as the mobile phase resulted in R_f values of 0.58 and 0.17, respectively. The product had a melting point of 133−136 °C and was identified as 2-naphthylacetic acid *N*-hydroxysuccinimide ester by ^{1}H-NMR analysis performed in deuterated chloroform. Signals were identified at 7.3−7.9 (7H), 4.104 (2H), and 2.785 (4H) representing naphthyl, methylene, and *N*-hydroxysuccinyl protons, respectively.

Synthesis of 2-Naphthylfucosylated Biantennary (Nap-Bi). Asialyl core fucosylated biantennary oligosaccharides were isolated from porcine fibrinogen and the reducing ends (5 μmol) were converted to an oligosaccharide-glycosylamine by reaction with ammonium bicarbonate as described previously (Silva et al., 1994). The oligosaccharide-glycosylamine reacted with 2-naphthylacetic acid *N*-hydroxysuccinimide ester (283 mg, 1 mmol) in 1 mL of DMF containing 5 μL of triethylamine. The reaction proceeded for 3 h at 50 °C and was terminated by the addition of 4 mL of 1 M sodium hydroxide and then stirred for 1 h. The excess 2-naphthylacetic acid was extracted four times with 4 mL of chloroform and the aqueous phase was applied to a Sephadex G-25 column (2.5 × 50 cm) eluted with pyridine−acetic acid buffer (0.5:0.5 v/v%) while monitoring $A_{280\ nm}$ (0.2 aufs). The naphthyl-derivatized oligosaccharides eluted between 98 and 154 mL and were pooled and freeze dried. A coupling yield of 80% was estimated by resolving the product peak from reducing oligosaccharides on HPAEC eluted isocratically with 20 mM sodium acetate in 100 mM sodium hydroxide detecting electrochemically with PAD. The major oligosaccharide product (Nap-Bi) was purified to homogeneity by injecting 500 nmol portions onto a PRP-1

[1] Abbreviations: RPHPLC, reverse-phase high-pressure liquid chromatography; FABMS, fast atom bombardment mass spectroscopy; DCC, dicyclohexylcarbodiimide; ^{1}H-NMR, proton nuclear magnetic resonance; TFA, trifluoroacetic acid; HPAEC, high-pressure anion exchange chromatography; PAD, pulsed amperometric detection; FWHM, full width at half-maximum height; aufs, absorbance units at full scale.

column (305 × 7.0 mm) eluted isocratically at 3 mL/min with 0.1% acetic acid and 14% acetonitrile while monitoring $A_{268\ nm}$ (0.5 aufs). Nap-Bi eluted at 23 min and was collected, freeze dried, and analyzed by ^{1}H-NMR and FABMS. The isolated yield of Nap-Bi was 2.5 μmol (50%) as determined by quantitative glucosamine analysis (Hardy et al., 1988).

Synthesis of Dansyl-Naphthyl-Biantennary (Dan-Nap-Bi). Nap-Bi (1 μmol) was dissolved in 100 μL of 100 mM sodium phosphate buffer pH 7.0, and incubated with galactose oxidase (60 μL, 60 units) and catalase (40 μL, 40 units) at 37 °C. The reaction was monitored by RPHPLC on a C-8 column eluting at 1 mL/min with 0.1% acetic acid and 12% acetonitrile while detecting naphthyl fluorescence (excitation 270 nm and emission 335 nm). At 2.5 h the reaction contained approximately 66% mono-oxidized, 33% dioxidized, and 33% unoxidzed Nap-Bi at which time the reaction was terminated by heating at 100 °C for 15 min.

Dansyl was directly coupled to the oxidized Nap-Bi products by adding dansyl ethylenediamine (20 μmol in 1 mL of 200 mM sodium phosphate buffer, pH 6.0) to 1 μmol of oligosaccharide. After 1 h at room temperature reductive amination was performed with pyridine borane (5 μL) followed by incubation at 37 °C for 18 h. Three 1 μmol reactions were combined and applied to a Sephadex G-25 column (50 × 1.5 cm) eluted with 100 mM acetic acid while monitoring $A_{280\ nm}$ (2 aufs). The first peak (50−85 mL) contained Nap-Bi and monodansylated Nap-Bi oligosaccharides and the second peak (90−100 mL) consisted of the didansylated Nap-Bi. The first G-25 fraction was resolved into three peaks on a C18 RPHPLC column (25 × 2 cm) eluting at 10 mL/min with 0.1% TFA and a step gradient of acetonitrile (18% for 15 min, 22% for 55 min, and 50% for 5 min) while monitoring $A_{268\ nm}$ (0.1 aufs). The second G-25 fraction was purified from a C18 RPHPLC column (25 × 1 cm) eluted at 3 mL/min with 0.1% TFA and a gradient of 20%−40% acetonitrile over 40 min while monitoring $A_{268\ nm}$ (0.2 aufs). Each purified Dan-Nap-Bi oligosaccharide was analyzed by ^{1}H-NMR and FABMS. Prior to energy transfer experiments oligosaccharides were prepared to 100% purity by isolation from a PRP-1 RPHPLC column eluting at 3 mL/min with 0.1% acetic acid and an acetonitrile gradient (15%−30% over 20 min).

Exoglycosidase Trimming and Periodate Oxidation of Fluorescent Oligosaccharides. Nap-Bi and monodansylated Nap-Bi oligosaccharides (50 nmol in 0.1 M sodium citrate phosphate buffer, pH 4.3) were treated with α-fucosidase (50 μL, 0.06 units) for 2 h at 37 °C. The defucosylated oligosaccharides were purified on a PRP-1 RPHPLC column as described above. The purified products were analyzed for monosaccharides to verify the complete loss of fucose (Hardy et al., 1988).

The underivatized antenna was trimmed enzymatically from each monodansylated Nap-Bi oligosaccharide. β-Galactosidase (30 μL, 0.05 units), β-acetyl hexosaminidase (2 μL, 0.8 units) and α-mannosidase (7 μL, 2.8 units) were added sequentially at 2 h intervals to 200 μL of monodansylated Nap-Bi (250 nmol) in 100 mM sodium phosphate citrate buffer, pH 4.3, and incubated at 37 °C. The reaction was monitored by RPHPLC on C18 eluted isocratically with 19% acetonitrile and 0.1% TFA while detecting the fluorescence of naphthyl. The retention time increased by 1−2 min as Gal, GlcNAc, and Man were removed. The trimmed oligosaccharides were purified on a polymer PRP-1 column as described above and analyzed by ^{1}H-NMR.

^{1}H-NMR and FABMS Characterization of Fluorescent Oligosaccharides. Each oligosaccharide (1−0.2 μmol) was buffered with 10 μL of 100 mM sodium phosphate, pH 7.0, and freeze dried. The sample was then exchanged three times with deuterium oxide and finally dissolved in 0.5 mL of 99.96% deuterium oxide containing 0.01% acetone as an internal standard (2.225 ppm). Spectra were acquired on a Bruker 500 MHz spectrometer at 30 °C and processed using Felix software (Hare Research, Eugene, OR).

FABMS was performed by adding 2 μL of α-monothioglycerol to the oligosaccharide (2 nmol in 10 μL of water) followed by Speed-Vac evaporation of the water. The sample was applied to the probe of a Finnigan Matt 900 FABMS operated in the positive mode.

Steady-State Energy Transfer Measurements. Nap-Bi and monodansylated Nap-Bi oligosaccharides (40 nmol) were dissolved in 3 mL of 5 mM sodium phosphate buffer, pH 7.0. The samples were analyzed for equimolarity by quantitative glucosamine analysis (Hardy et al., 1988). Steady-state fluorescence energy transfer measurements were made on a Perkin Elmer LS-50B luminescence spectrometer by exciting naphthyl at 272 nm while monitoring emission at 335 nm. The steady-state efficiencies (E) were calculated from the quench of naphthyl at 335 nm according to eq 1,

$$E = \left(1 - \frac{F_{DA}}{F_D}\right) \tag{1}$$

where F_{DA} was the fluorescence intensity of monodansylated Nap-Bi and F_D was the fluorescence intensity of Nap-Bi at 335 nm. The Förster distance of 50% energy transfer efficiency determined by eq 2

$$R_0^6 = 78 \times 10^{-5} \kappa^2 \phi J n^{-4} \tag{2}$$

used an orientation factor (κ^2) of $^2/_3$ assuming the donor and acceptor pair are randomly orientated (Englert & Leclerc, 1978; Haas et al., 1978). The refractive index ($n = 1.4$), donor quantum yield ($\phi = 0.095$), and overlap integral ($J = 5.61 \times 10^{13}$ cm^{-1} M^{-1} nm) were the same as determined previously resulting in an R_o value of 20.8 Å (Rice et al., 1991). The steady-state distance $\bar{r}$ between donor and acceptor was determined by the Förster eq 3.

$$\bar{r} = R_o \left(\frac{1 - E}{E}\right)^{1/6} \tag{3}$$

Time-Resolved Energy Transfer Measurements. The fluorescence decay of Nap-Bi and monodansylated Nap-Bi oligosaccharides were measured using a time-correlated single-photon counting apparatus. A cavity-dumped Rhodamine 6-G dye laser was the excitation source that was synchronously pumped by a mode-locked, frequency-doubled Nd:YAG laser. The 570 nm wavelength from Rhodamine 6G dye laser was amplified at megahertz repetition rates by a six-pass amplifier pumped by a argon ion laser and then frequency doubled by an angle-tuned KDP crystal (Weaver et al., 1993). The resulting 285 nm excitation wavelength was the exciting source. The emission was monitored at 355 nm and was dispersed by a subtractive mode double monochromator with an extremely small temporal dispersion and a spectral resolution of 2 nm. Signals were detected by

a Hamamatsu R-2809U-07 microchannel plate PMT with an overall instrument response of 55 ps at full width at half-maximum height (FWHM). A scattering dry milk solution was used to collect the instrument response function. Measurements were made from 0 to 40 °C with increments of 10 °C. Duplicate decays were performed at each temperature. Because of the increased power of the excitation only a short data collection time was needed. The average acquisition time for each decay was around 10 min with the peak channel reaching 20 000 counts at a time resolution of 60 ps/channel. Due to some photosensitivity, the decay curves initially obtained for monodansylated Nap-Bi oligosaccharides could not be fitted to the energy transfer model. This problem was solved by stirring samples with a magnetic stirring bar during data acquisition.

Data Analysis. The fluorescence decay of Nap-Bi and monodansylated-Nap-Bi were analyzed in terms of the sum of the exponential, which is defined by

$$I_D(t) = \sum \alpha_i \exp\left(-\frac{t}{\tau_i}\right) \quad (4)$$

where the α_i and τ_i are the amplitude and the lifetime of the *i*th component, respectively. The goodness of the fits was judged by the value of reduced χ^2, the weighted residuals, and the autocorrelation of the residuals (Bevington, 1969; Grinvald & Steinberg, 1974; O'Conner & Phillips, 1984). For time-correlated single-photon counting, the probability of observing any photon emission was given by the Poisson probability function (Bevington, 1969). Therefore, χ^2 should be close to 1.0 for a good fit. The steady-state distances were determined from time-resolved measurements by calculating *E* according to eq 1 after substituting the average lifetime of Nap-Bi ($\langle\tau_D\rangle$) for F_D and that of the monodansylated Nap-Bi ($\langle\tau_{DA}\rangle$) for F_{DA}.

To determine the distribution of donor−acceptor distances, the fluorescence decay can be described as

$$I_{DA}(t) = \sum a_k \int P_k(r) \sum \alpha_i \exp\left\{-\frac{t}{\tau_i}\left[1 + \left(\frac{R_o}{r}\right)^6\right]\right\} dr \quad (5)$$

where $I_{DA}(t)$ is the decay of donor in the presence of an intramolecular acceptor and the first summation indicates the number of the distance populations. $P_k(r)$ is the population function, and a_k is the amplitude of the *k*th population. A Lorentzian function, eq 6, was used as a probability distribution in our study

$$P_k(r) = \frac{1}{\pi} \frac{\sigma_k}{(r - \langle r_k\rangle)^2 + \sigma_k^2} \quad (6)$$

where σ_k is the standard deviation for the function and FWHM equals $2\sigma_k$. In eq 5, α_i and τ_i are the amplitude and the lifetime, respectively, of the donor in the absence of acceptor, which were obtained by fitting the decays to exponentials as described in eq 4 and were fixed in the analysis. The fits were performed on a VAX station M76 computer and judged as described above such that all final χ^2 values fell between 0.99 and 1.22. The floating parameters were a_k, $\langle r_k\rangle$, and s_k, which define the relative intensity, distance, and shape of the *k*th population, respectively. The amplitude of the distribution was normalized to 1, and the fitted distance was integrated from $0.4R_o$ to $2.2R_o$ in $0.1R_o$ increments, which virtually covers the whole range of the possible energy transfer distance.

Table 1: Mass Spectral[a] Analysis of Fluorescent Oligosaccharides

structure[b]	calcd. mass[c]	obsd mass	calcd composition
I	1976.7[d]	1976.6	$Gal_2Man_3GlcNAc_4FucNap$
II	2231.2	2229.6	$DanGal_2Man_3GlcNAc_4FucNap$
III	2231.2	2230.6	$DanGal_2Man_3GlcNAc_4FucNap$
IV	2506.6	2505.8	$Dan_2Gal_2Man_3GlcNAc_4FucNap$

[a] Performed by FABMS. [b] See Figure 3 for structures **I**−**VI**. [c] Predicted average mass ($M + 1$). [d] Major ion was M + Na.

RESULTS

Synthesis of Fluorescent Oligosaccharides. A new synthetic approach to prepare fluorescent biantennary oligosaccharides is outlined in Figure 1. Asialyl biantennary oligosaccharides obtained from porcine fibrinogen were converted to the oligosaccharide-glycosylamine. These were coupled to 2-naphthylacetic acid to form a glycosylamide linkage between naphthyl and GlcNAc 1 (Figure 1A). The coupling of naphthyl proceeded with high yield (80%) and anomeric purity (>95%), as determined by ^{1}H-NMR analysis of the isolated product. This result was identical to that determined previously when coupling tyrosine to an oligosaccharide-glycosylamine (Tamura et al, 1994; Silva et al., 1994a,b). Therefore, the steric bulk of naphthyl did not influence the reaction as previously noted for dansyl chloride coupling to a glycosylamine of GlcNAc (Manger et al., 1992). The desired Nap-Bi oligosaccharide (**I**) was purified from RPHPLC (Figure 2A) with an acceptable isolation yield (50%) and was used as a synthon for generating monodansylated Nap-Bi energy transfer probes.

Galactose oxidase was used to introduce an aldehyde at the C-6 hydroxyl on the terminal Gal residues of **I** (Figure 1B). Monitoring the reaction by RPHPLC allowed termination when the monoaldehyde peak was the major product (Figure 2B). The partially oxidized oligosaccharides were reductively aminated with dansyl ethylenediamine resulting in a mixture consisting of four products which could be resolved by RPHPLC (Figure 2C).

On the basis of the relative elution order, fluorescence and absorbance spectra, and molecular weight determined by mass spectrometry (Table 1), the four products were tentatively identified as Nap-Bi (**I**), isomeric monodansylated Nap-Bi (**II** and **III**), and didansylated Nap-Bi (**IV**) (Figure 3). Starting with 6 μmol of **I** the synthesis yielded approximately 0.5 μmol of the desired oligosaccharides **II** and **III**.

Proton NMR was used to verify these structures and to distinguish between isomers **II** and **III**. The anomeric and *N*-acetyl signals of oligosaccharides **I**−**IV** are shown in Figure 4, and chemical shifts are listed in Table 2. Oligosaccharides **I**−**IV** gave rise to a doublet at δ 5.012−4.996 with a coupling constant (J_{1-2}) of 9.7 Hz which is consistent with a β-glycosylamide linkage between GlcNAc 1 and naphthyl. The structural reporter group signals for GlcNAc 1, 2, and Fuc 1′ of **I** were shifted due to the influence of the ring anisotropy of naphthyl, but other reporter group signals were in close agreement with those reported for a core-fucosylated biantennary oligosaccharide (Spellman et al., 1991; Silva et al., 1994a).

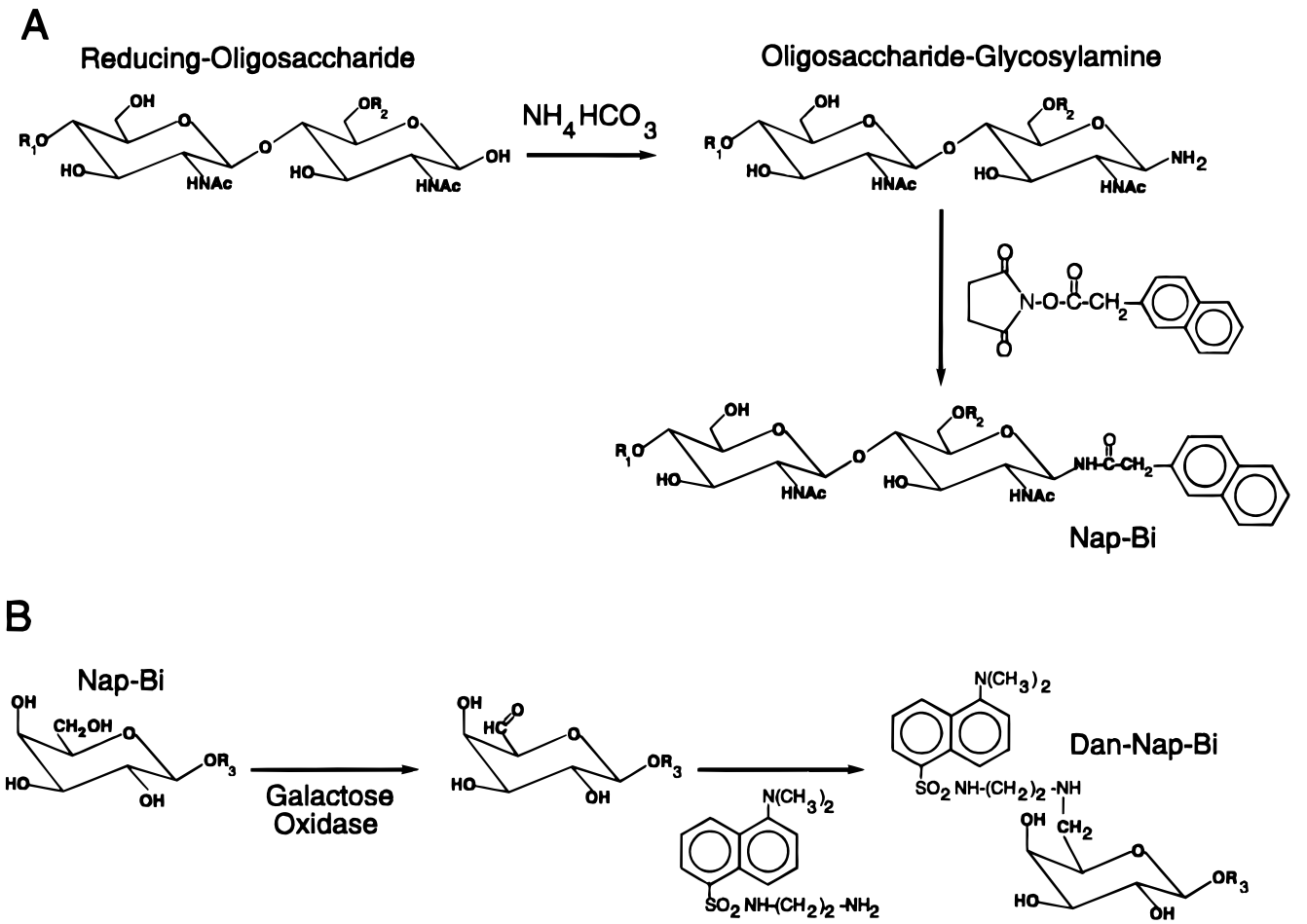

FIGURE 1: Derivatization of N-linked biantennary with donor and acceptor fluorophores. (A) Reducing oligosaccharides reacted with ammonium bicarbonate to form oligosaccharide-glycosylamines. These coupled with 2-naphthylacetic acid *N*-hydroxysuccinimide ester resulting in the covalent attachment of naphthyl to GlcNAc 1 via a β-glycosylamide linkage. (B) Following RPHPLC purification of Nap-Bi (Figure 2), galactose oxidase acted on the nonreducing end Gal residues of Nap-Bi resulting in the formation of an aldehyde at position C-6. Dansyl ethylenediamine coupled to C-6 by reductive amination using pyridine borane as the reducing agent, and the isomers were resolved by HPLC. R^1 is the nonreducing portion of the biantennary oligosaccharide, R^2 is fucose, and R^3 is the reducing-end portion of the biantennary oligosaccharide.

Attachment of dansyl ethylenediamine to the C-6 of Gal on **II** and **III** caused a single Gal anomeric proton signal to shift upfield into the bulk region of the spectrum (3.4−4 ppm) precluding its assignment by ^{1}H-NMR. Comparison of the remaining Gal anomeric proton on either **II** or **III** with those of **I** allowed their tentative assignment as Gal 6′ and 6 despite the finding that these signals were also shifted slightly (0.004 ppm) upfield (Figure 4). The absence of Gal anomeric signals for oligosaccharide **IV** supported the proposal that attachment of dansyl to a Gal causes a dramatic shift in the anomeric protons.

The anomeric protons of GlcNAc 5 and 5′ were also shifted upfield (0.009 ppm in **II** and 0.040 ppm in **III**) due to the attachment of dansyl to an adjacent Gal residue (Figure 4). Due to the coincident chemical shift of the anomeric protons of GlcNAc 5 and 5′ signals in the spectrum of **I**, it was not possible to assign these signals in the spectra of oligosaccharides **II** and **III**.

The spectra for **II** and **III** also demonstrated an upfield shift for one of the *N*-acetyl protons of GlcNAc 5 and 5′ (0.052−0.072 ppm) (Table 2). However, due to chemical shift perturbations (0.002−0.004) observed for the remaining signal, the unambiguous assignment of these resonances as either 5 or 5′ in oligosaccharides **II** and **III** was not possible and could not be used as criteria for the structural assignment of **II** and **III**. A number of new signals also appear in the spectra of **II**−**IV** which may belong to Gal or GlcNAc ring protons that are shifted downfield from the bulk region due to the strong ring current of dansyl (Figure 4).

However, the anomeric protons for Man 4 and 4′ were readily discernable in **II** and **III** and were selected as markers in the following experiments aimed at distinguishing between isomers. Exoglycosidase trimming of the underivatized antenna of **II** and **III** was used to differentiate between the isomers. Trimming was successful for oligosaccharide **III**, resulting in a product having an NMR spectra that demonstrated the loss of anomeric proton associated with Man 4 as well as those proposed for GlcNAc 5 and Gal 6 (data not shown). However, the exoglycosidase trimming of isomer **II** failed to remove the final Man despite repeated attempts using an excess of α-mannosidase. This was circumvented by trimming Fuc 1′ prior to removing Gal 6′, GlcNAc 5′, and Man 4′. The NMR spectra of the trimmed product of **II** verified the complete loss of the Man anomeric signal associated with 4′ and the retention of the signal for 4. These results allowed assignment of isomer **II** and **III** as shown in Figure 3 and also confirmed the tentative assignments of resonances for GlcNAc and Gal as shown in Figure 4.

Oligosaccharides **II** and **III** were defucosylated to generate isomers **V** and **VI** (Figure 3). These were characterized by

Table 2: Proton NMR[a] Chemical Shifts for Fluorescent Oligosaccharides

proton[b]	I	II	III	IV
H-1 of				
1	5.012	5.015	4.996	5.009
1′	4.852	4.850	4.829	4.838
2	4.656	4.644	4.620	4.641
4	5.116	5.112	5.108	5.100
4′	4.917	4.902	4.905	4.901
5	4.576	4.576	4.572	4.587
5′	4.576	4.576	4.536	4.574
6	4.465	nd[c]	4.459	nd
6′	4.469	4.465	nd	nd
H-2 of				
3	4.236	4.209	4.218	4.211
4	4.186	4.178	4.180	4.178
4′	4.099	4.092	4.083	4.092
H-6 of				
1′	1.097	1.098	1.080	1.091
N-Ac of				
1	1.639	1.639	1.635	1.639
2	2.080	2.080	2.049	2.057
5	2.046	1.994	2.042	1.999
5′	2.042	2.038	1.970	1.994

[a] Values are the chemical shift in ppm relative to acetone (2.225 ppm) at 30 °C. [b] See Figure 3 for structure and residue nomenclature. [c] nd indicates the signal was not detected.

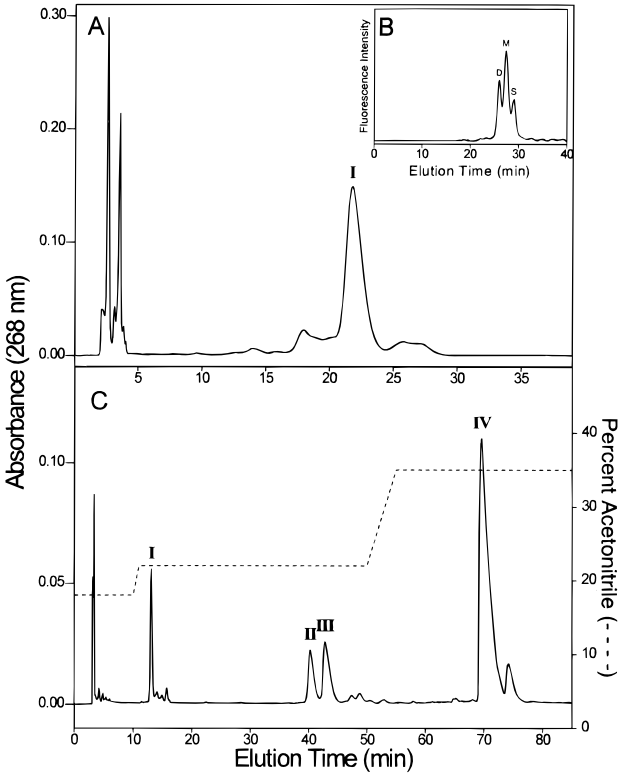

FIGURE 2: RPHPLC separation of fluorescent oligosaccharides. (A) The product of naphthyl coupling to fibrinogen oligosaccharides was resolved on a PRP-1 polymer RPHPLC column eluting at a flow rate of 3 mL/min with 0.1% acetic acid and 14% acetonitrile while monitoring $A_{268\ nm}$ (0.5 aufs). The major product (**I**) was isolated and identified as the β-glycosylamide of Nap-Bi. (B) The galactose oxidase reaction was monitored by RPHPLC eluted isocratically at 1 mL/min with 0.1% acetic acid and 12% acetonitrile while detecting Nap-Bi fluorescence. The chromatogram illustrates the product ratio at 2.5 h where S is starting material, M is monooxidized Nap-Bi, and D is dioxidized Nap-Bi. (C) Following reductive amination with dansyl ethylenediamine, products were resolved on C-18 RPHPLC (1 × 25 cm) eluting at 3 mL/min with 0.1% TFA and a step gradient of acetonitrile (18% for 10 min, 22% for 40 min, 22%−35% for 5 min, and 35% for 30 min) while monitoring A_{268nm} (0.2 aufs). The major peaks were identified as oligosaccharides **I**−**IV** as shown in Figure 3.

monosaccharide analysis which verified the loss of a fucose residue. The resulting fluorescently labeled biantennary oligosaccharides were analyzed in fluorescence energy transfer experiments and compared to **II** and **III** to determine the influence of core fucosylation on conformation.

Fluorescence Energy Transfer Measurements. Fluorescence energy transfer was used to determine both the average (steady-state) and distribution of distances (time-resolved) separating the two fluorophores in **II** and **III**. The average donor−acceptor distances were determined using both steady-state and time-resolved measurements. Donor quenching established that naphthyl was quenched to a greater extent in **III** relative to that of **II**. This resulted in an average donor−acceptor distance of 21.6 and 18.9 Å for **II** and **III**, respectively. Furthermore, steady-state distances determined by either donor quenching or time-resolved energy transfer were within 0.5 Å.

Time-resolved energy transfer data was used to further explore the distribution of donor−acceptor distances of **II** and **III**. The fluorescence decay of the donor was monitored at temperatures ranging from 0 to 40 °C. Both 2-naphthylacetic acid and **I** produced a fluorescent decay with a major component (95%) of 36 ns and a minor component (5%) of 3 ns. The removal of the core fucose had a negligible influence on the lifetime of the donor. These results were comparable to those reported previously when studying triantennary glycopeptide, except the lifetimes of the major and minor components were 27 ns (95%) and 5 ns (5%), respectively (Rice et al., 1991). Both components were taken into account when the decays were fitted to a distance population.

The presence of a single acceptor fluorophore in **II** and **III** resulted in a decrease in the donor's lifetime and its conversion to a multiexponential decay. Nonlinear least squares fitting was used to analyze the decay curve and solve for the distance $\bar{r}$, amplitude (A), and FWHM (σ) for either one or two donor−acceptor distance populations. An example of the measured fluorescence decay curve and the nonlinear least squares fit is shown in Figure 5. The decay curves were first fitted using a single Lorentzian distribution (Figure 5A). Analysis of the autocorrelation, residuals, and χ^2 allowed an assessment of the goodness of the fit (Bevington, 1969; Grinvald & Steinberg, 1974; O'Conner & Phillips, 1984). In cases where a single distribution gave an unsatisfactory fit, the decay curve was fitted using two Lorentzian distributions (Figure 5B).

A single Lorentzian distribution was sufficient to fit the decay curves of **II** over the temperature range 0−40 °C (Figure 6A, Table 3). When the temperature was changed from 0 to 40 °C, the population shifted to a shorter mean distance by nearly 2 Å. This minor change in distance may arise from either an increased rotation of the fluorophores at an elevated temperature, resulting in a further randomization of k^2 or an actual shortening of the donor−acceptor distance by 2 Å.

In contrast, two distribution populations were required to fit the decay curves for **III** (Figure 6B, Table 3). At each temperature between 0 and 40 °C a minor (25%) short

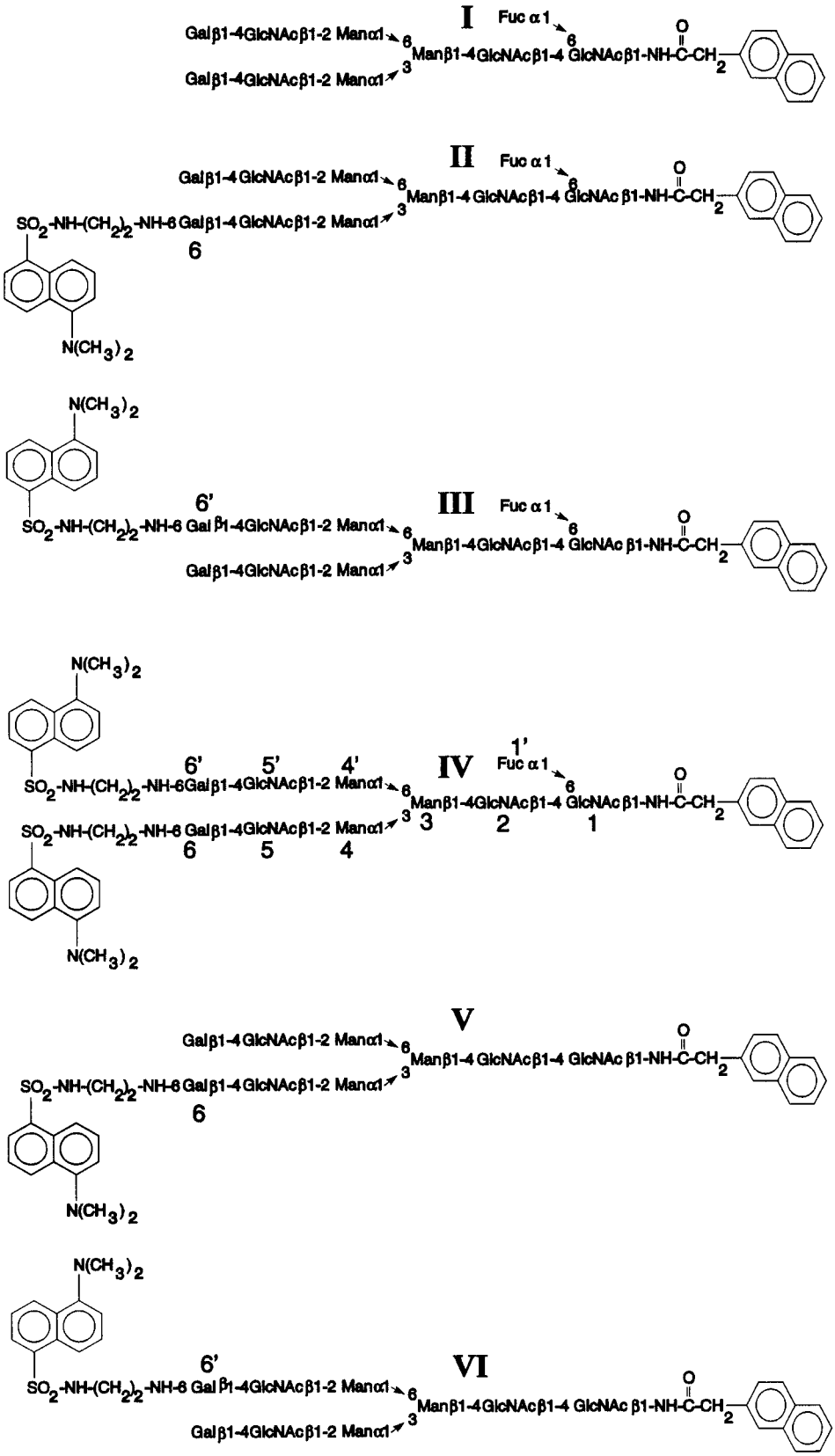

FIGURE 3: Structures of fluorescent oligosaccharides. The structures of Nap Bi (**I**), isomeric monodansylated Nap-Bi (**II** and **III**), and didansylated Nap-Bi (**IV**) are shown. The attachment of dansyl ethylenediamine to either Gal 6 or Gal 6′ in **II** and **III** was established by NMR and FABMS. Oligosaccharides **V** and **VI** were derived from **II** and **III** by trimming with α-fucosidase. The residue nomenclature discussed in the text is presented on structure **IV**.

donor−acceptor distance population (11.5 Å) and a major (75%) long donor−acceptor distance population (20.5 Å) were determined (Figure 6B, Table 3). The amplitudes of these two populations were not influenced by temperature modulation, but the mean distance shifted slightly (2 Å) to a shorter distance with increasing temperature.

To explore further the influence of core fucosylation on oligosaccharides conformation, **II** and **III** were compared

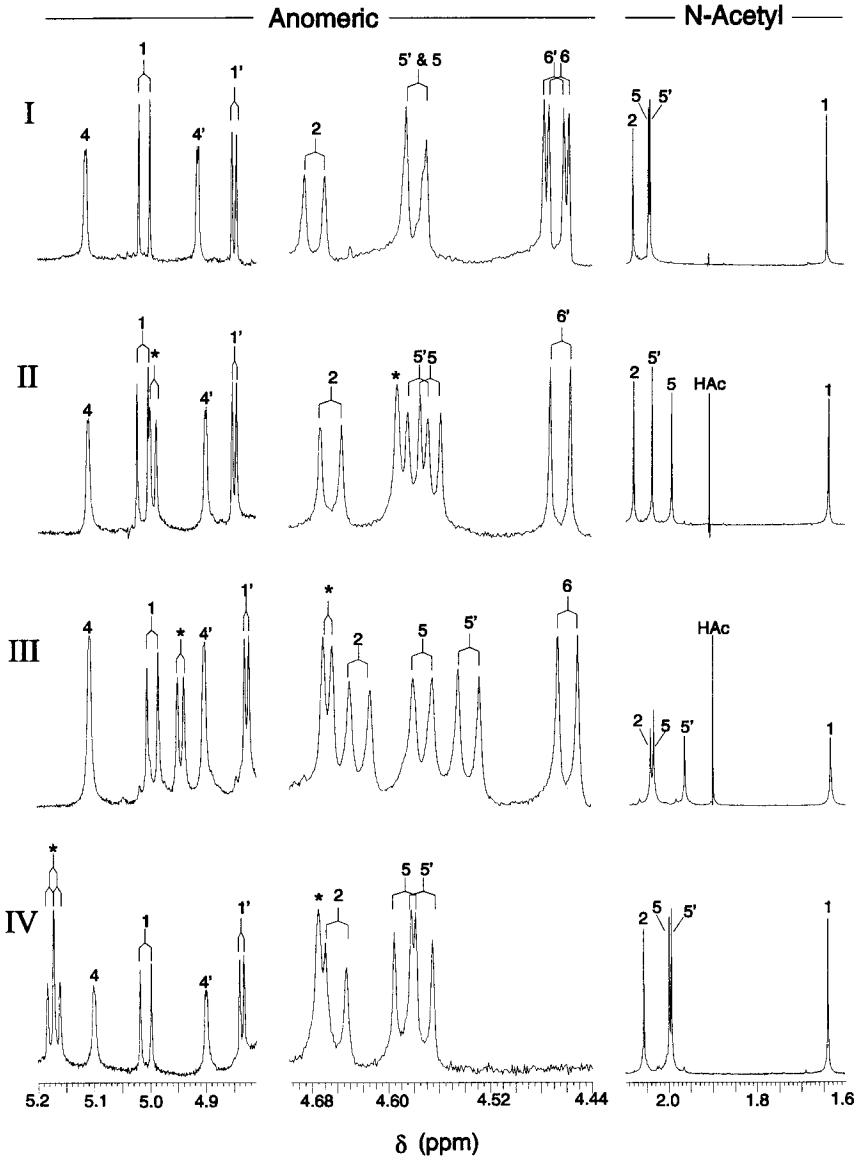

FIGURE 4: Partial ^{1}H-NMR spectra of oligosaccharides **I**−**IV**. The structural reporter group regions for GlcNAc 1 and Man anomeric protons (5.2−4.8 ppm), GlcNAc 2, 5, 5′, and Gal anomeric protons (4.68−4.44 ppm), and the *N*-acetyl protons (2.1−1.6 ppm) are shown. Resonances identified with an asterisk denote signals of the oligosaccharide that were shifted downfield due to the ring anisotropy effect of dansyl.

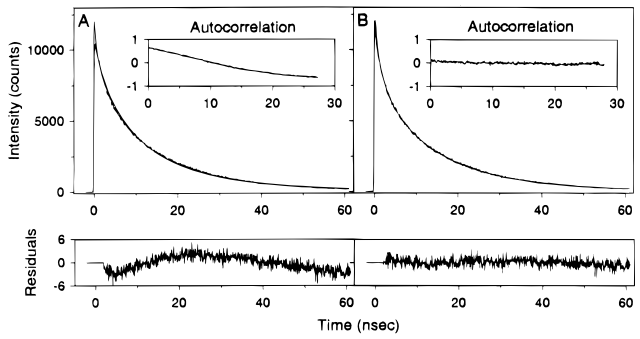

FIGURE 5: Time-resolved fluorescence energy transfer. (A) The fluorescence decay curve of **III** acquired at 20 °C and the nonlinear least squares fit of the data using a single Lorentzian population is shown. Both the autocorrelation and plot of the residuals indicate a poor fit to the experimental data. (B) The result of fitting the same decay curve using two Lorentzian distributions, resulting in an autocorrelation and a plot of residuals that indicated a good fit of the experimental data ($\chi^2 = 1.1$).

to **V** and **VI**. Steady-state energy transfer measurements indicated that the average donor−acceptor distance of **V** and **VI** were unaffected by the removal of fucose. Furthermore, time-resolved measurements established that isomers **II** and **V** shared a nearly identical donor−acceptor distance distributions at each temperature, illustrating that the absence of core fucose did not cause the Gal 6 antenna to fold to a shorter distance population (Figure 6A,C, Table 3).

However, the trimming of fucose had a dramatic effect on oligosaccharide **VI** (Figure 6D, Table 3). This isomer still exhibited two donor−acceptor populations, but following removal of fucose the amplitudes of the two populations were strongly modulated by temperature. At 40 °C the longer population had an amplitude of nearly 70% and the shorter nearly 30%, whereas at 0 °C the populations had nearly equivalent amplitudes.

The temperature dependent conformational equilibrium of **VI** allowed estimation of the values associated with the thermodynamics of antenna flexibility. The ratio of the amplitude of the longer versus the shorter donor−acceptor distance was plotted versus the inverse temperature which gave a regression line where the slope is $-\Delta H/R$ and the

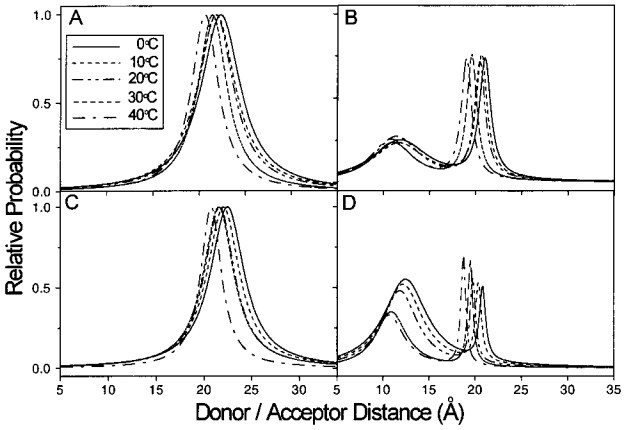

FIGURE 6: Time-resolved donor−acceptor distance distributions. Deconvoluted time-resolved decay of naphthyl in oligosaccharides **II**, **III**, **V**, and **VI** at 0−40 °C are shown in panels A−D, respectively. Oligosaccharide **II** (A) displayed a single population of donor−acceptor distances (22 Å) at all temperatures, whereas **III** (B) displayed two populations representing extended (20.5 Å) and folded (11.5 Å) conformers. Following the removal of fucose, oligosaccharide **V** (C) displayed the same population distribution as determined for **II** in panel A. However, on removal of fucose from **III** to form oligosaccharide **VI** (D), the ratio of extended and folded conformations was modulated by temperature. At 0 °C the ratio was nearly 1:1, whereas at 40 °C the extended conformer represented 70% and the folded conformer represented 30%.

Table 3: Time-Resolved Energy Transfer Measurement of Oligosaccharides **II**, **III**, **V**, and **VI**

temp (°C)	mean[a] distance (Å)	amplitude[b]	FWHM[a] (Å)	mean distance (Å)	amplitude	FWHM (Å)
	Oligosaccharide **II**[d]			Oligosaccharide **III**		
0	22.3	1.00	5.22	21.0	0.74	1.50
				11.8	0.26	7.43
10	21.8	1.00	50.4	20.6	0.76	1.46
				11.7	0.24	7.08
20	21.8	1.00	4.64	20.6	0.72	1.42
				11.4	0.28	6.24
30	21.4	1.00	3.86	19.6	0.76	1.33
				11.0	0.24	5.63
40	20.6	1.00	3.56	19.0	0.74	1.35
				10.8	0.26	5.15
	Oligosaccharide **V**			Oligosaccharide **VI**		
0	22.4	1.00	4.34	20.8	0.45	0.80
				12.4	0.55	5.79
10	22.0	1.00	4.16	20.3	0.48	0.76
				12.1	0.52	5.42
20	21.6	1.00	3.84	19.7	0.52	0.70
				11.8	0.48	4.70
30	21.5	1.00	3.88	19.5	0.65	0.66
				10.9	0.35	4.04
40	20.7	1.00	2.66	18.7	0.67	0.62
				10.7	0.33	3.97

[a] Calculated from eq 1 using average τ values from eq 4. [b] Value is the a_k determined from eq 5. [c] Value is $2\sigma_k$ determined from eq 6. [d] See Figure 3 for structures.

intercept is $\Delta S/R$ (Figure 7). By comparison, the slope was close to zero for **III**, whereas the calculated enthalpy and entropy of the conformational change for **VI** were 4.25 kcal/mol and 14.99 cal/mol·K, respectively.

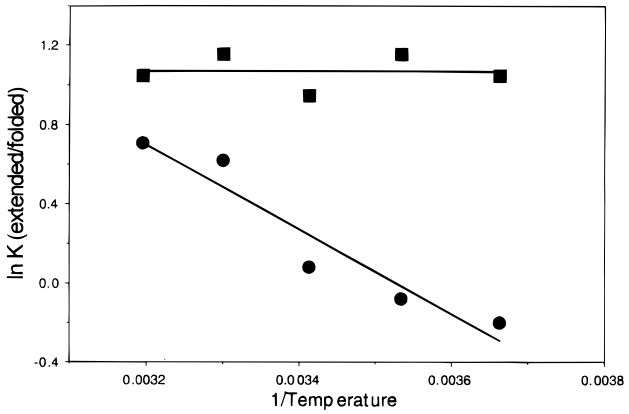

FIGURE 7: Thermodynamic analysis of antenna flexibility. The ratio of amplitude of the extended/folded conformations was plotted versus the inverse temperature to obtain the slope ($-\Delta H/R$) and intercept ($\Delta S/R$) for oligosaccharide **VI** (●). This is compared with the inflexibility of **III** containing core fucose (■). The results establish a ΔH of 4.25 kcal/mol and a ΔS of 14.99 cal/mol·×d7K for **VI**.

DISCUSSION

A. Synthesis and Characterization of Fluorescent Oligosaccharides. Fluorescence energy transfer was used to analyze the solution conformations of an N-linked biantennary oligosaccharide. This technique has been frequently applied to study distances in proteins and nucleic acids but has only recently found application in examining the flexibility of N-linked oligosaccharides (Rice et al., 1991; Wu & Brand, 1994). One of the challenges in using energy transfer to examine oligosaccharide conformations is in developing efficient synthetic strategies that incorporate two extrinsic fluorophores into defined locations in the molecule. Previously, this was accomplished with a triantennary glycopeptide using the amine terminus as a site for attaching a donor fluorophore. However, because of the variation in peptide sequence of glycopeptides isolated from different glycoproteins, the direct comparison of the conformational properties of different N-linked oligosaccharides attached to different peptides may introduce ambiguity into the experiment. The present study has improved on the fluorophore-labeling scheme by attaching the donor directly to the reducing end, allowing direct comparison of energy transfer data on N-linked oligosaccharides derived from different glycoprotein sources.

The synthetic scheme employed successfully coupled 2-naphthylacetic acid to the glycosylamine of GlcNAc 1, resulting in a stable β-glycosylamide linkage. This coupling reaction proceeded with high yields despite the presence of a core fucose residue which potentially could sterically block the reactive center. Therefore, the glycosylamine-coupling chemistry described here appears to be advantageous for introducing a fluorophore into N-linked oligosaccharides despite previous reports of its complications (Manger et al., 1992).

A second improvement in the derivatization strategy was to couple dansyl ethylenediamine directly to partially oxidized oligosaccharide **I**. This modification shortened the synthesis of dilabeled oligosaccharides by avoiding the purification and characterization of individual oligosaccharide-hydrazones as previously performed for triantennary glycopeptides (Rice & Lee, 1990). This proved to be an efficient process that resulted in the chromatographic resolution of oligosaccharides **II** and **III**, each of which contains a single uniquely located dansyl fluorophore.

However, direct NMR assignment was complicated due to overlapping signals creating ambiguity in the assignment

of isomers **II** and **III**. Many signals were shifted due to the influence of the ring anisotropy of the dansyl group attached to a terminal galactose. Identification of the dansyl-labeling site was only possible after enzymatically trimming the underivatized antenna. However, even this approach was met with difficulty due to the α-mannosidase resistance of Man 4′ on isomer **II**. Only following removal of Fuc 1′ was this residue was susceptible to α-mannosidase cleavage.

B. Distance Measurements by Fluorescence Energy Transfer. The fluorescence energy transfer properties of oligosaccharides **II** and **III** were readily distinguished even by steady-state analysis. Isomer **II** produced a longer donor−acceptor distance (21.6 Å) compared to the shorter average distance (18.9 Å) determined for **III** (Table 3). These data compare favorably with the steady-state measurements on similar antenna found in a triantennary glycopeptide, thereby indicating that the attachment of naphthyl directly to GlcNAc 1 still provides distances that are close to R_o (20.8 Å) for this donor−acceptor pair (Rice et al., 1991).

Time-resolved energy transfer was used to investigate the flexibility of **II** and **III**. A single donor−acceptor distance population was sufficient to fit the decay curve of **II**, and temperature modulation failed to perturb the conformation of the Gal 6 antenna which was apparently fixed in an extended conformation. This is in contrast to the results observed for the same antenna located on a triantennary N-linked glycopeptide which displayed both an extended population at 23 Å and a folded population at 10 Å in which the relative amplitudes were modulated by temperature (Rice et al., 1991; Wu et al 1993). Thus it can be concluded that the conformation of the Gal 6 antenna is strongly influenced by the presence or absence of a third antenna. The GlcNAcβ1-2Man linkage of the Manα1-3Man antenna has been identified as a potential site of flexibility in modeling studies of core-fucosylated biantennary (Mazurier et al., 1991). On the basis of results presented here, it is hypothesized that this GlcNAcβ1-2Man linkage in a biantennary projects the antenna in an extended conformation. Whereas the additional presence of a GlcNAcβ1-4 linkage to Man 4, as in a triantennary structure, perturbs the conformation of the adjacent GlcNAcβ1-2, causing folding of the Gal 6 antenna. It is also evident from the data presented for **V** that core fucosylation has no effect on the conformation of the Gal 6 antenna in biantennary but could potentially cause modulation of the flexibility of this antenna in triantennary.

Analysis of the flexibility of **III** established the presence of two populations of donor−acceptor distances. The longer distance population (19 Å) corresponds to an extended antenna, whereas the shorter distance (10 Å) represents a folded conformer. The ratio of extended to folded conformers was not perturbed by temperature modulation. However, following the removal of fucose from the core to generate **VI**, the flexibility increased and the ratio of extended and folded conformers was strongly influenced by temperature modulation. The flexibility of the Gal 6′ antenna in **VI** is similar to that observed for the same antenna in a triantennary glycopeptide (Wu et al, 1991). At 0 °C a nearly equal ratio of extended and folded conformers exist, whereas at higher temperatures the extended conformer dominates. The site of flexibility in this antenna is probably the Manα1-6Man linkage as previously suggested (Rice et al., 1991; Mazurier et al., 1991).

The modulation of extended and folded conformation in **VI** allowed estimation of thermodynamic parameters associated with antenna folding. The positive entropy of unfolding indicates a loss of order when the oligosaccharide extends. Likewise, a positive enthalpy indicated that thermal energy allows the antenna to occupy a higher energy conformation when extended. The magnitudes of ΔH (4.25 kcal/mol versus 7.1 kcal/mol) and ΔS were comparable (14.9 cal/mol·K versus 25.8 cal/mol·K) but not identical to the values determined for the Gal 6′ antenna in a triantennary glycopeptide (Wu et al., 1991). The differences may reflect subtle alterations in this antenna depending on the presence or absence of the third antenna or may result from the difference in synthetic design between these two experiments.

The importance of core fucose in the binding of an N-linked biantennary oligosaccharide to a plant lectin has recently been demonstrated (Bourne et al., 1994). It was shown that Fuc 1′ had a high contact area with the lectin (Bourne et al., 1994) and that the absence of fucose led to binding of the oligosaccharide in such a way that the Manα1-3Man linkage was in a high-energy conformation (Bourne et al., 1992). The results presented here also reveal a role for core fucosylation in stabilizing the extended conformation of the Gal 6′ antenna, presumably by sterically blocking the folded conformation, making it less energetically favorable.

Admittedly, the attachment of the fluorophores to oligosaccharides required for fluorescent energy transfer measurements could potentially create artifactual conformations. However, the results presented here and in previous studies suggest the contribution from the fluorophore is negligible in that the major differences in conformation are dependent on the individual antenna under investigation. Also, no other techniques currently in use can provide long-range distance information, report on antenna flexibility, and allow estimation of the thermodynamics of the conformational equilibrium. These attributes make fluorescence energy transfer a powerful and attractive approach to study N-linked oligosaccharide conformations.

ACKNOWLEDGMENT

The authors acknowledge technical assistance provided by Manpreet Wadhwa, Tamara McBroom, and Pengguang Wu.

REFERENCES

Bevington, P. R. (1969) *Data Reduction and Error Analysis for the Physical Sciences*, McGraw-Hill Book Company, New York.
Bourne, Y., Rougé, P., & Cambillau, C. (1992) *J. Biol. Chem. 267*, 197−203.
Bourne, Y., Mazurier, J. Legrand, D., Rougé, P., Montreuil, J., Spik, G., & Cambillau, C. (1994) *Structure 2*, 209−219.
Brisson, J. R., & Carver, J. P. (1983) *Biochemistry 22*, 3680−3686.
Carver J. P. (1991) *Curr. Opin. Struct. Biol. 1*, 716−720.
Cheetum, J. C., Artymiuk, P. J., & Phillips., D. C. (1992) *J. Mol. Biol. 224*, 613−628.
Childs, R. A., Fezei, T., Yuen, C-T., Drickamer, K., & Quesenberry, M. S. (1990) *J. Biol. Chem. 265*, 20770−20777.
Cygler, M., Rose, D. E., & Bundle, D. R. (1991) *Science 253*, 442−445.
Englert, A., & Lerclerc, M. (1978) *Proc. Natl. Acad. Sci. U.S.A. 75*, 1050−1051.
Grinvald, A., & Steinberg, T. Z. (1974) *Anal. Biochem. 59*, 583−598.
Haas, E. Katchalski-Katzir, E., & Steinberg, I. Z. *Biopolymers 17*, 11−31.
Hardy, M. R., Townsend, R. R., & Lee, Y. C. (1988) *Anal. Biochem. 170*, 54−62.

Homans, S. W., & Rutherford T. (1993) *Biochem. Soc. Trans. 21*, 449−452.
Homans, S. W., Dwek, R. A., Fernandes, D. L., & Rademacher, T. W. (1983) *FEBS 164*, 231−235.
Imberty, A., Tran, V., & Perez, S. (1989) *J. Comput. Chem. 11*, 205−216.
Jardetsky, O. (1980) *Biochim. Biophys. Acta 621*, 227−232.
Koča, J. Perez, S., & Imberty, A. (1995) *J. Comput. Chem. 16*, 296−310.
Lee, Y. C. (1992) *FASEB J. 6*, 3193−3200.
Manger, I. D., Rademacher, T. W., & Dwek, R. A. (1992) *Biochemistry 31*, 10724−10732.
Mazurier, J., Dauchez, M., Vergoten, G., Montreuil, J., & Spik, G. (1991) *Glycoconjugate J. 8*, 390−399.
O'Conner, D. V., & Phillips, D. (1984) *Time-Correlated Single-Photon Counting*, Academic Press, New York.
Rice, K. G., & Lee, Y. C. (1990) *J. Biol. Chem. 265*, 18423−18428.
Rice, K. G., Wu, P., Brand, L., & Lee, Y. C. (1991) *Biochemistry 30*, 6646−6655.
Rice, K. G., Wu, P., Brand, L., & Lee, Y. C. (1993) *Biochemistry 32*, 7264−7270.
Rice, K. G., Wu, P., Brand, L., & Lee, Y. C. (1994) *Curr. Opin. Struct. Biol. 3*, 669−674.
Rutherford, T. J., Partridge, J., Weller, C. T., & Homans, S. W. (1993) *Biochemistry 32*, 12715−12724.
Silva, M., Tamura, T., McBroom, T., & Rice, K. G. (1994a) *Arch. Biochem. Biophys. 312*, 151−157.
Silva, M., Tamura, T., & Rice, K. G. (1994b) *Arch. Biochem. Biophys. 315*, 460−466.
Spellman, M. W., Leonard, C. K., Basa, L. J., Gelineo, J., & van Halbeek, H. (1991) *Biochemistry 30*, 2395−2406.
Sharon, N. (1984) *TIBS 9*, 198−202.
Sharon, N. (1993) *TIBS 18*, 221−226.
Tamura, T., Wadhwa, M. S., & Rice, K. G. (1994) *Anal. Biochem. 216*, 335−344.
Tvaroska, I., Imberty, A., & Pérez, S. (1990) *Biopolymers 30*, 369−379.
Weaver, W. L., Iwata, K., & Gustafson, T. L. (1993) *J. Opt. Soc. Am. 10*, 852−857.
Weis, W. I., Drickamer, K., & Henderson, W. A. (1992) *Nature 360*, 127−134.
Wu, P., Rice, K. G., Brand L., & Lee Y. C. (1991) *Proc. Natl. Acad. Sci. U.S.A.* 88, 9355−9359.
Wu, P., & Brand, L. (1994) *Anal. Biochem. 21*8, 1−13.

BI9513719